Journal of
Mechanical
Science and
Technology

Journal of Mechanical Science and Technology 21 (2007) 2023~2030

Micromechanics analysis of progressive failure in cross-ply carbon fiber/epoxy composite under uniaxial loading

Suparerk Sirivedin, Seog Young Han* and Kwan Soo Lee

School of Mechanical Engineering, Hanyang University, Haengdang-Dong, Seongdong-Gu, Seoul, 133-791, Korea

(Manuscript Received April 11, 2007; Revised October 18, 2007; Accepted October 18, 2007)

Abstract

Three-dimensional micromechanics models were created for cross-ply carbon fiber/epoxy composite with a layer stacking-sequence arranged in $[0/90]_s$. Elasto-plastic finite element (FE) analysis was performed to study the effects of thermal residual stress and the stress redistribution as individual fiber fractures. The modified Rice and Tracey (RT) void growth model was used to predict the location of transverse matrix crack. The stress amplification factors (SAF) in intact fibers adjacent to a fractured fiber were calculated and compared with the planar array composite. The FE results show that small defects have already formed in curing process, and ply-delamination is likely to occur near the corner of free-edges. The transverse matrix crack was predicted to occur near the fiber fracture location in the models having little inter-fiber spacing.

Keywords: Carbon fibers; Finite element; Matrix cracking; Stress concentrations

1. Introduction

Catastrophic failure of a composite may begin from microscopic events such as fiber fracture, matrix crack, interface debonding. The stress concentration around a fiber fracture increases the axial stress of the nearest neighboring intact fibers, and can lead to fracture in the near future. The stress concentration and the inter-fiber spacing are the key factors governing failure of a composite. In previous work, the stress amplification factors (SAFs) of unidirectional composite systems have been determined [1, 2]. Zhang et al. [3] described the inability of classical lamination theory (CLT) to accurately predict stress state in three-dimensional models. They proposed numerical and analytic solutions to examine the effect of free-edge and ply-cracking. Wagner and Eitan [4] proposed an analytic solution to calculate the stress concentration factor in two-dimensional composites. They assumed that the additional tensile stress in the adjacent intact fiber is induced by the surrounding shear stress in the matrix, as a result of fiber fracture. Zhou and Wagner [5] extended their previous work by assuming a certain debonded length to occur in a broken fiber in their model. However, the plasticity dissipation was disregarded in all mentioned models. Xia, Chen and Ellyin [6] used a representative volume element (RVE) in finite element analysis to study damage in $[0/90_3/0]_T$ glass-fiber/epoxy composite. They found that a damage zone forms in matrix material on the free surface along the length of fibers. Katerelos, McCartney and Galiotis [7] used laser Raman spectroscopy (LRS) to obtain the strain magnification factor (SMF) for Kevlar® fiber-epoxy composite. They also observed a transverse matrix crack near the fiber fracture location. The transverse matrix crack was also observed in the other cross-ply polymer composites [8, 9].

Several authors have used micro-scale finite element models to study failure in variety of cross-ply composites [10-12]. Unfortunately, no attempt has been made to obtain SAF for cross-ply polymer composites. In this work the cross-ply composite with a

*Corresponding author. Tel.: +82 2 2220 1895, Fax.: +82 2 2298 4634
E-mail address: syhan@hanyang.ac.kr

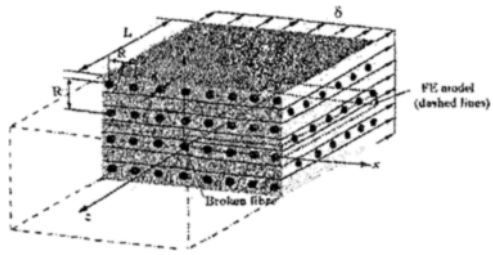

Fig. 1. Micromechanics-based finite element model.

layer stacking-sequence arranged in [0/90]s was studied (see Fig. 1).

2. Failure prediction in cross-ply composite

2.1 Stress amplification factor (SAF)

The effect of stress concentration around a fiber fracture can be quantified by using a stress amplification factor [1], which is defined as

$$SAF = \frac{\sigma_{peak}}{\sigma_{far}} \tag{1}$$

where σ_{peak} is the peak value of the axial fiber stress in the adjacent fibers and σ_{far} is the axial fiber stress in the far field. Zhou and Wagner [5] mentioned that this factor can be decomposed as

$$SAF = 1 + \frac{\sigma_{add}}{\sigma_{far}} \tag{2}$$

where σ_{add} is the additional stress in the adjacent fibers, which is induced by shear stress in matrix material. Once the value of SAF is known, the amount of additional axial stress in the intact fibers can be estimated by Eq. (2).

2.2 Ductile fracture based on void growth model

Sirivedin [13] observed small voids formed in the epoxy specimen (see Fig. 2). The dog-bone specimens were made by silicone mould. All fabrication processes were performed in the vacuum chamber with a degassing time of half an hour. However, small voids were still found in the specimen. The void size depends on the fabrication process employed. Hull and Clyne [14] mentioned in their book that small voids often form in the region adjacent to the

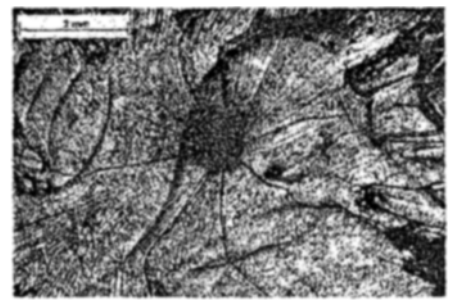

Fig. 2. Fractography of specimen shows small voids in epoxy.

fibers, especially in the interfacial area, and also in the matrix-rich pockets or the fiber-free regions between laminae. In ductile fracture, the local plastic strain is a key parameter determining the mechanism of fracture caused by micro-void nucleation, growth, and coalescence. To deal with the problem involving multi-loading conditions, the equivalent or effective plastic strain $\bar{\varepsilon}_p$ [15] is often used to assess the development of plastic strain in the local region, which is given by

$$\bar{\varepsilon}_p = \int_0^t \sqrt{\frac{2}{9}\left[\left(d\varepsilon_1^p - d\varepsilon_2^p\right)^2 + \left(d\varepsilon_2^p - d\varepsilon_3^p\right)^2 + \left(d\varepsilon_3^p - d\varepsilon_1^p\right)^2\right]}\,dt \tag{3}$$

where $d\varepsilon_1^p$, $d\varepsilon_2^p$, $d\varepsilon_3^p$ are the principal components of an increment of plastic strain and dt is the time increment. If this equivalent plastic strain exceeds the critical fracture strain of the material, the crack will propagate. The growth rate of micro-voids ahead of the crack tip is sensitive to the mean stress in this region. If the mean stress is negative, void closure leads to an increase in the effective fracture strength of the material. Based on the RT void-growth criterion [16], the critical fracture strain in a high triaxial stress field ahead of the crack tip can be expressed as

$$\varepsilon_f^* = \frac{\ln\left(\frac{d_p}{D_p}\right)}{0.283\exp\left(1.5\sigma_m/\bar{\sigma}\right)} \tag{4}$$

where d_p is the critical void spacing, D_p is the critical void size (see Fig. 3), σ_m is the mean stress, $\bar{\sigma}$ is the von Mises stress, and the constant value 0.283 approximated from the case of highest triaxiality [16]. In practice, the critical void size and void

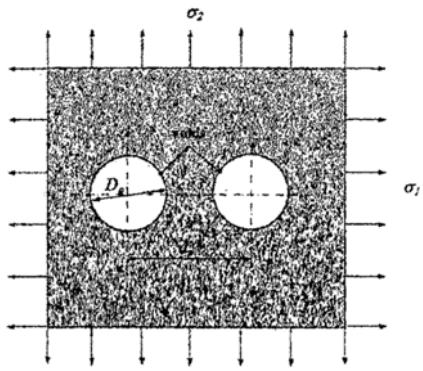

Fig. 3. Two-dimensional void nucleation, growth and coalescence diagram.

spacing are difficult parameters to measure and in order to evaluate their ratio, reference is made to the tensile test. If failure occurs in the tensile test, where $\bar{\sigma} = \sigma$ and $\sigma_m = \sigma/3$, when $\varepsilon_f^* = \varepsilon_{fi}$ [17] the ratio of the critical void spacing to void size in Eq. (4) is then given by

$$\ln\left(\frac{d_p}{D_p}\right) = 0.283\varepsilon_{fi}\exp(0.5) \tag{5}$$

Substitution of Eq. (5) into Eq. (4) gives the critical fracture strain as

$$\varepsilon_f^* = \frac{1.648\varepsilon_{fi}}{\exp(1.5\sigma_m/\bar{\sigma})} \qquad \text{provided } \sigma_m \rangle\ 0 \tag{6}$$

The critical fracture strain in Eq. (6) is valid provided the value of the mean stress is positive. Hence, ductile fracture will occur when

$$\bar{\varepsilon}_p = \varepsilon_f^* \tag{7}$$

where $\bar{\varepsilon}_p$ is the equivalent plastic strain which is obtained from Eq. (3) and ε_f^* is the critical plastic strain obtained from Eq. (6).

3. Micromechanics-based finite element models

The effect of the inter-fiber spacing on the stress redistribution near the fiber fracture location was examined by varying the ratio R/d, where R is the fiber center distance and d is the fiber diameter (see Fig. 1). By exploiting symmetries, the problem was modeled by using a quarter section of the actual specimen (see Fig. 4). The ratios of R/d of 1.1, 1.2, 1.3, 1.5, 2, 3, 4, and 5 are of interest. The finite element (FE) models were created for those ratios by using 24,576 eight-node linear brick elements. In order to obtain accurate FE results for small R/d ratios, the simulations for the R/d of 1.1 and 1.2 were resumed by using the fine-mesh FE model comprised of 41,472 linear brick elements. The FE analysis was divided up into the following sequence of ABAQUS® load steps:

(i) *Thermal pre-load*: A temperature drop of $\Delta T = -60\ ^\circ C$ was applied to simulate the curing process. It has been shown in the previous work [1] that the value of temperature drop agreed well with experiment [14].

(ii) *Applied mechanical load*: A uniform displacement δ corresponding to an applied strain of 0.4 % on the composite was imposed at every node on the end face of the composite (see Fig. 4). Experiments have shown that first fracture occurs at approximately this level of applied strain [18].

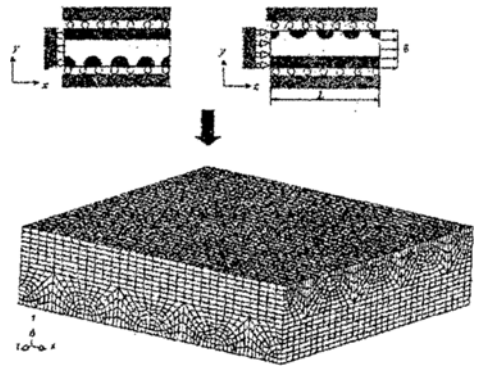

Fig. 4. Finite element model & mesh.

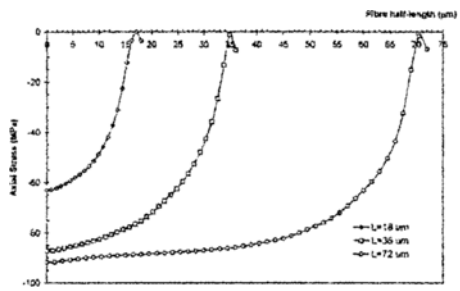

Fig. 5. Effect of fiber length on the variation of axial stresses in cross-ply fiber at R/d = 1.5 in the fiber fracture load step.

Table 1. Material properties of carbon fiber and epoxy matrix.

Material properties	Carbon fiber	Matrix LY5052/HY5052 (relaxed properties)
Axial Tensile Modulus, GPa	392	1.78
Transverse Modulus, GPa	20	1.78
Axial Tensile Strength, GPa	3.2*(fracture)*	31×10^{-3} *(yield)*
Axial Fracture Strain,%	0.8	4.2
Transverse Poisson's ratio, $\nu_{R\theta}$	0.27	0.36
Poisson's ratio in R-Z direction, ν_{RZ}	0.03	0.36
Axial Coefficient of Thermal Expansion, K^{-1}	-0.25×10^{-6}	58×10^{-6}
Transverse Coefficient of Thermal Expansion, K^{-1}	25×10^{-6}	58×10^{-6}

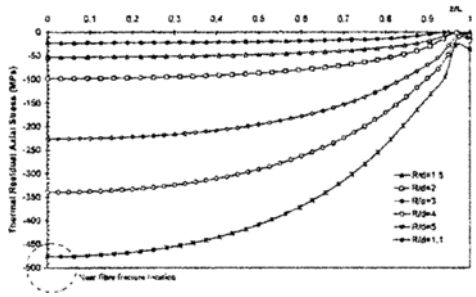

Fig. 6. Effect of thermal residual stress on variation of cross-ply fiber stresses.

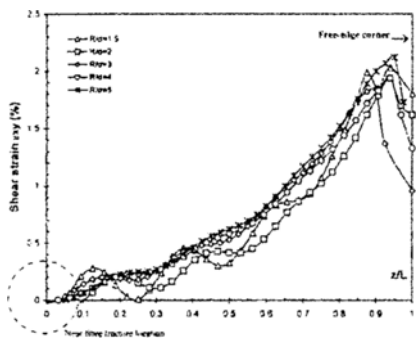

Fig. 7. Variation of Interlaminar shear strains in epoxy matrix along the stress free boundary.

(iii) *Fiber fracture*: Fiber fracture was simulated by removing all displacement constraints on the fiber-end face to form a penny-shaped crack. This was achieved by ramping the forces on the fiber-end face linearly down to zero within the time-step defined in ABAQUS®. The applied strain of 0.4% was held constant during this step.

The high-modulus M40-3k-40® carbon fibers (Toray Industries) used in the model are transversely isotropic and were assumed to be linear elastic (see

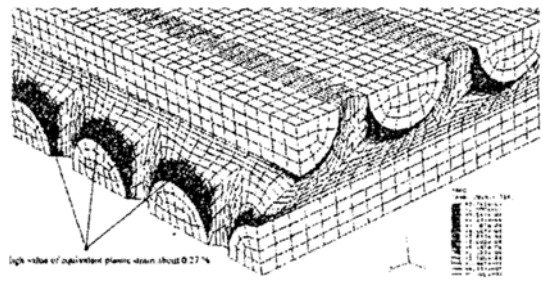

Fig. 8. The equivalent plastic strain developed in epoxy matrix near the fiber ends during fabrication

Table 1). However, since carbon fiber has orientation-dependent mechanical properties, the feature in ABAQUS® has enabled locally defining the material orientation for fibers in the models correctly. The elasto-plastic behavior of matrix material was modeled by using the relaxed properties of LY5052/HY5052® (Ciba-Geigy) epoxy. The strain rate used for the LRS measurements was approximately $0.25\times10^{-2}\,\mathrm{min}^{-1}$.

4. Results and discussion

4.1 Effect of thermal residual stress

Fabrication of the composite specimen induces thermal residual stresses. This is due to a coefficient of thermal expansion mismatch between carbon fiber and epoxy matrix. Since the coefficient of thermal expansion of epoxy is higher than that of the carbon fiber, the larger contraction of the matrix puts the fibers into compression, and also induces localized yielding at the fiber ends on the free edges. To examine the effect of thermal residual stress by micromechanics analysis, it is necessary to be aware of the effect of free edges. The micromechanics models for

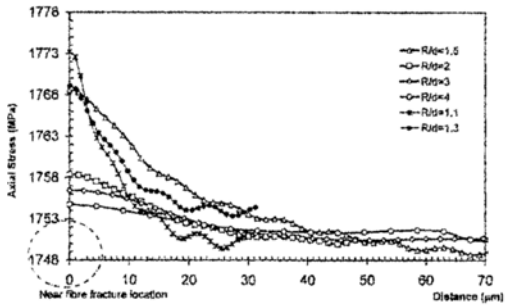

Fig. 9. Effect of fiber fracture on the variation of axial stresses in intact fibers.

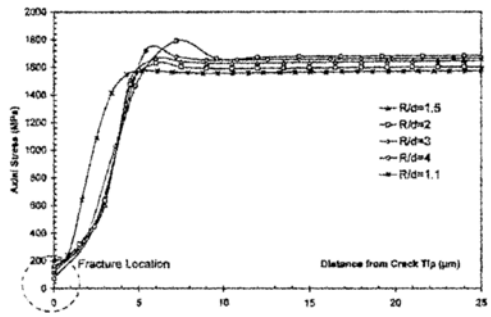

Fig. 11. Variation of axial stresses in a broken fiber with inter-fiber spacing.

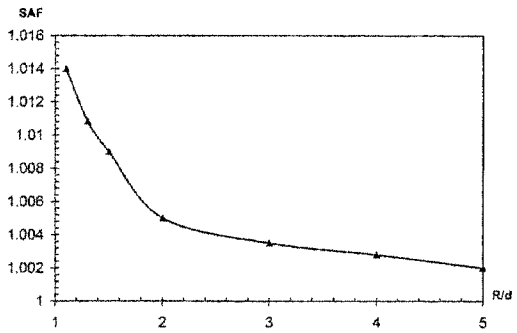

Fig. 10. Effect of fiber fracture on variation of SAFs with inter-fiber spacing.

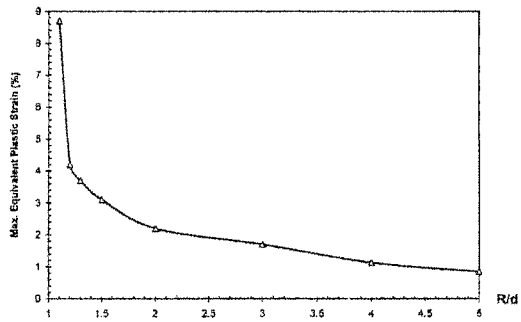

Fig. 12. Effect of fiber fracture on variation of the equivalent plastic strains with inter- fiber spacing.

R/d ratio of 1.5 with different dimensions were used to validate the minimum fiber half-length required in the model. As shown in Fig. 5, the maximum value of thermal residual stresses was of the same order for the fiber half-lengths of $36\mu m$ and $72\mu m$. Hence, the micromechanics model must have a fiber half-length at least six times greater than its diameter. As can be seen in Fig. 6, larger inter-fiber spacing results in an increase of the thermal residual stress.

4.2 Effect of free edges

The layer stacking-sequence in this work was arranged in [0/90]s, i.e., the fiber orientation of the second ply is in the transverse direction to the fibers in the first ply. This may lead to free-edge distortion when the composite is subjected to thermal load. Consequently, the curing process also induced interlaminar shear stress between plies. Since the epoxy is ductile, it would be advantageous to use the interlaminar shear strain to quantify failure in the epoxy matrix. An interlaminar shear strain of about 2% was found near the corner of the free edge for all cases at the thermal pre-load simulation step (see Fig. 7). This is the reason for the non-zero stress at the ends of fibers in Fig. 5. It has been found also that an equivalent plastic strain of 0.2% was developed in the same area. This may imply that delamination will take place in this location if there is any further increase in applied loading.

As a result of larger matrix shrinkage along the free edges, plastic strain has developed in the matrix material near the fiber ends (see Fig. 8). It should be noted that the initial defects were formed in the composite during fabrication process.

4.3 Stress amplification factors in cross-ply composite under uniaxial loading

When an individual fiber breaks, the load carried by the broken fiber is then transferred through the matrix. Subsequently, the shear stress in the matrix induces the extra stress in the neighboring intact fibers. Failure in the intact fibers can be quantified by using the stress amplification factor (SAF) as defined in Eq. 1. The axial stress of the nearest neighboring intact fiber in the stress of the nearest neighboring intact fiber in the model with R/d ratio of 1.1 was

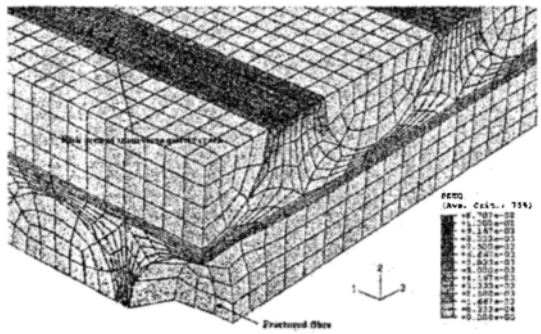

Fig. 13. High value of the equivalent plastic strain developed in a pocket space between the cross-ply fibers.

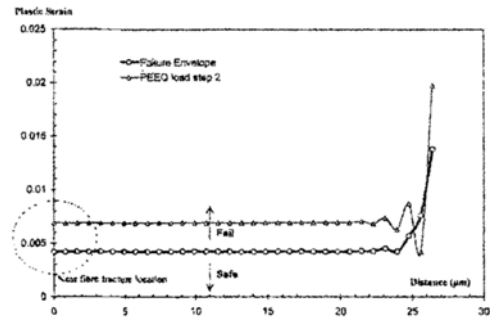

Fig. 14. Prediction of transverse matrix crack based on modified RT model, R/d =1.1.

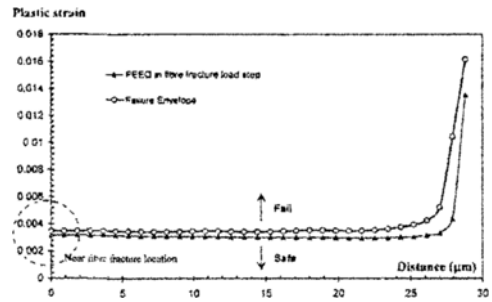

Fig. 15. Prediction of transverse matrix crack based on modified RT model, R/d =1.2.

found to increase by 1.4 % to the far-field stress (see Fig. 9). In previous work [1], the axial stress of the nearest neighboring fiber in the planar array composite at the same R/d ratio was found to increase by 38 %. The results from both studies show that the cross-ply fibers assist in carrying the load broadened out by the broken fiber. The stress amplification factors were calculated and plotted in Fig. 10. In contrast to the planar array composite, the axial stresses in a broken fiber in cross-ply composite are fairly similar for all ratios (see Fig. 11).

4.4 Failure in epoxy matrix

A high value of the equivalent plastic strain, ranging from 1-8.7 % was found in matrix material between the cross-ply fibers due to fiber fracture (see Fig. 12). As the R/d ratio increases from 1.1 to 1.5, the value of the equivalent plastic strain decreases precipitously. When R/d ratio is greater than 2, the equivalent plastic strain reduces gradually. The high value of the equivalent plastic strain that developed between the inter-fiber spacing between cross-ply fibers may indicate a risk area of transverse matrix crack (see Fig. 13). As mentioned earlier in section 2.2, small voids often form in matrix-rich pockets. Therefore, a modified RT void-growth model was used to predict the fracture location in epoxy matrix. The maximum values of stresses at every nodal point along the fiber half-length in a pocket space between cross-ply fibers were used to compute the critical fracture strain envelope from Eq. 6. The values were then compared with the curve of equivalent plastic strain PEEQ obtained at the same location. By making use of this criterion, it has been found in the model with R/d ratio of 1.1 that the transverse matrix crack has already taken place in a pocket space between cross-ply fibers since a certain amount of uniform displacement was applied in the second load step (see Fig. 14). As can also be seen in Fig. 14, the averaged value of equivalent plastic strain is greater than the fracture strain of about 64 %. This may imply that a transverse matrix crack was formed at the early stage of applied mechanical load step. Failure prediction for the model with R/d ratio of 1.2 is shown in Fig. 15; the equivalent plastic strain curve has partially contacted the fracture strain envelope near the fracture location at the end of the fiber fracture simulation step (i.e., the last load step). The initiation location of transverse matrix crack is likely to occur at the touching point of the two curves. Apart from these two models, based on this criterion, no fracture was found in the other R/d ratios at this applied mechanical strain level.

5. Conclusions

The FE results show that small defects had already formed in epoxy matrix near the fiber ends on the free-edges in the curing process. Due to the thermal effect, an interlaminar plastic strain was developed in the matrix region near the corner of free-edges which

would have led to ply-delamination when a certain amount of mechanical load was applied. The fiber fracture in cross-ply composite has less effect on inducement of the additional axial stress in the nearest intact fiber compared to the planar array composite. Based on the modified RT void growth model, transverse matrix crack was predicted near the fiber fracture location in the models having little inter-fiber space between cross-ply fibers.

Acknowledgments

This work was supported by the Second Brain Korea 21 Project in 2007, funded by the Ministry of Education and Human Resources Development of the Korean government. The first author (S. Sirivedin) would like to thank Prof. Costas Galiotis, Dr. David N. Fenner and Dr. Rajat B. Nath for useful information and discussion.

Nomenclature

σ_{peak} : Peak value of the axial fiber stress
σ_{far} : Far fixed axial fiber stress
σ_{add} : Additional stress in the adjacent fibers
$\bar{\varepsilon}_p$: Equivalent or effective plastic strain
$d\varepsilon_i^p$, : Principal components of an increment of plastic strain
dt : Time increment
d_p : Critical void spacing
D_p : Critical void size
σ_m : Mean stress
$\bar{\sigma}$: Von Mises stress
ε_f^* : Critical plastic strain

References

[1] S. Sirivedin, D. N. Fenner R. B. Nath and C. Galiotis, Effect of inter-fiber spacing and matrix cracks on stress amplification factors in carbon-fiber/epoxy matrix composites. Part I: planar array of fibers, *Composites Part A.* 34 (12) (2003) 1227-1234.

[2] S. Sirivedin, D. N. Fenner, R. B. Nath and C. Galiotis, Effect of inter-fiber spacing and matrix cracks on stress amplification factors in carbon-fiber/epoxy matrix composites. Part II: hexagonal array of fibers, *Composites Part A.* 37 (11) (2006) 1936-1943.

[3] D. Zhang, J. Ye and H. Y. Hong, Free-edge and ply cracking effect in cross-ply laminated composites under uniform extension and thermal loading, *Compos. Struct.* 76 (4) (2006) 314-325.

[4] H. D. Wagner and A. Eitan Stress concentration factors in two-dimensional composites: effects of material and geometrical parameters, *Compos. Sci.Technol.* 46 (4) (1993) 353-362.

[5] X. F. Zhou and H. D. Wagner Stress concentrations caused by fiber failure in two-dimensional composites, *Compos. Sci. Techno.* 59 (7) (1999) 1063-1071.

[6] Z. Xia, Y. Chen and F. Ellyin, A meso/micromechanical model for damage progression in glass-fiber/epoxy cross-ply laminates by finite-element analysis, *Compos. Sci. Technol.* 60 (8) (2000) 1171-1179.

[7] DTG Keterelos, L. N. McCartney and C. Galiotis, Local strain re-distribution and stiffness degradation in cross-ply polymer composites under tension, *Acta Materialia.* 53 (12) (2005) 3335-3343.

[8] S. Choi and B. V. Sankar, Fracture toughness of transverse cracks in graphite/epoxy laminates at cryogenic conditions, *Composites Part B.* 38 (2007) 193-200.

[9] DTG Katerelos, P. Lundmark J. Varna and C. Galiptis, Analysis of matrix cracking in GFRP laminates using Raman spectroscopy, Compos. Sci. Technol. doi:10.1016/j.compscitech.2006.10.019., (2006).

[10] F. Ellyin, Z. Xia and Y. Chen, Viscoelastic micromechanical modeling of free edge and time effects in glass fiber/epoxy cross-ply laminates, *Composites Part A.* 33 (2002) 399-409.

[11] W. Sun, F. Lin and X. Hu, Computer-aided design and modelling of composite unit cells, *Compos. Sci. Technol.* 60 (2001) 289-299.

[12] T. Hobbiebrunken, M. Hojo, B. Fiedler, M. Tanaka, S. Ochiai and K. Schulte, Thermomechanical analysis of micromechanical formation of residual stresses and initial failure in CFRP, *Int. J. of JSME Series A.* 47 (3) (2004) 349-356.

[13] S. Sirivedin, Micromechanics of progressive failure in carbon fiber-reinforced composites using finite element method, PhD thesis, King's College London, University of London. (2001).

[14] D. Hull and T. W. Clyne, An introduction to composite materials, 2nd ed, Cambridge University Press, (1996).

[15] W. Johnson and P. B. Mellor, Engineering Plasticity, 2nd ed, Ellis Horwood Limited., (1983)

[16] J. R. Rice and D. M. Tracey, On the ductile enlargement of voids in triaxial stress fields, *J. Mech. Phys. Solids* 17 (1969) 201-217.

[17] N. P. O'Dowd, Advanced Fracture Mechanics: Lecture notes on Fundamentals of Elastic and Elastic-Plastic Fracture. Imperial College of Science Technology and Medicine, University of London. (1998).

[18] V. Chohan and C. Galiotis, Effects of interface, volume fraction and geometry on stress redistribution in polymer composites under tension, *Composites Science and Technology*. 57 (8) (1997) 1089-1101.